Journal of Materials Chemistry A

Accepted Manuscript

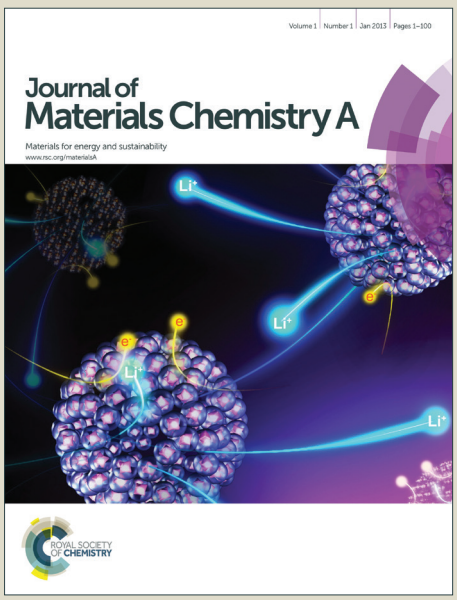

ROYAL SOCIETY OF CHEMISTRY

www.rsc.org/materialsA

Journal of
Materials Chemistry A

RSCPublishing

ARTICLE

New dry carbon nanotube coating of over-lithiated layered oxide cathode for lithium ion battery

Cite this: DOI: 10.1039/x0xx00000x

Received ooth January 2012,
Accepted ooth January 2012

DOI: 10.1039/x0xx00000x

www.rsc.org/

Junyoung Mun[a,b], Jin-Hwan Park[a], Wonchang Choi[c], Anass Benayad[a], Jun-Ho Park[a], Jae-Myung Lee[a], Seok-Gwang Doo[a] and Seung. M. Oh[d]

For cathode in lithium ion batteries, carbon is one of the best coating materials to solve two main problems which are surface deterioration and poor electrical conductivity. However, the conventional carbon coating procedures, chemical carbonization processes, are especially difficult to apply for oxide cathode, which could deteriorate the oxide structure. Here a new dry 100-nm-thick homogeneous multi-walled carbon nanotube (MWCNT) coating is prepared on the high-capacity oxide cathode material, $Li_{1.17}Ni_{0.17}Co_{0.1}Mn_{0.56}O_2$, by applying shear stress without breakdown of crystal structure and morphology of the cathode. The electronic conductivity of carbon composite with the coated sample is 170 mS cm^{-1} which is over 40 times as much as the value of the pristine cathode with the same amount of carbon. In addition, at high current condition of 2450 mA g^{-1}, 103 mAh g^{-1} of specific capacity is obtained even with only 3 percent of carbon in weight including the coated MWCNT. The unconventionally improved performances are explained by the suppression of the electronic resistance and surface charge transfer resistance by electrochemical analyses.

1. Introduction

In general, one of the main concerns in the lithium ion batteries (LIBs) is surface deteriorations including breakdown of surface crystal structure and formation of highly resistive passivation film caused by electrochemical side reaction between electrode and electrolyte.[1-4] This phenomena is inevitable because the voltage between positive and negative electrode is beyond the electrochemical stability window of the electrolyte to obtain high energy and power density. In this regard, surface coatings have been investigated for their ability to improve the stability of the surface of the electrode and to reduce the failure modes on the interface between the electrode and electrolyte. A great many studies have been proposed to address this issue, but most of studies are focusing on the coating of inorganic materials, such as metal oxides and metal fluorides because they are highly stable, but they could increase internal resistivity in the LIB because they are electrically non-conductive materials.[5-7] Concerning this, carbon is considered to be one of the best coating materials. It is highly conductive, electrochemically stable, easily prepared, abundant, environmentally friendly, and inexpensive. Kinetic hindrances and irreversible side reactions can be relieved by improving the electronic conductivity and passivating the active site on electrode material to the electrolyte via introducing the carbon coating. Hence a great deal of research has been carried out into the carbon coating of lithium ion battery electrodes in order to solve the above-mentioned problems. Carbon coatings on the active materials for LIBs have been achieved via chemical methods which are in-situ growing of the carbon coating during the active material synthesis and post-synthetic process such as chemical vapor deposition or carbon sputtering.[8,9] Among carbons, several allotropes of carbons like graphite and carbon nanotube, which have the repeated covalent bonding exhibit high electronic conductivity, and therefore, these conductive carbons are better suited for coating. However, the preparations of those kinds of carbons are limited because catalyst or synthesis condition of high temperature is essential for giving carbon a stacking order or crystallinity. Especially, the coatings of conductive carbon on the oxide cathode have been very restricted because of the chemically thermal side reactions between carbon and oxide at the elevated temperature, so called carbon thermal reduction. To date, carbon coating on the positive electrode materials of LIBs has been implemented for the polyanion-type materials such as $LiFePO_4$ and $LiCoPO_4$. For the oxide cathode materials, only few kinds of carbon

coating have been introduced by carbon sputtering, ball milling and co-precipitation method.[8, 10-12] However, they would be limited, as the carbon coating should be thin, homogeneous and highly conductive and additionally, the cathode morphology should be preserved after the coating.[13-15]

As an effort to increase the energy density of LIBs to enhance the use of LIBs for electric vehicle and smart grid, several positive electrode materials that show high capacity have been exploited. In this regard, one of the spotlighted positive electrode materials is the over-lithiated layered oxide (OLO, $Li_xMn_yCo_zNi_aO_2$, x>1.0) that gives larger specific capacity than those of $LiCoO_2$ and $LiMn_2O_4$ thanks to additional lithium ions in the transition metal site.[16-20] Nonetheless, this material is not used in practical LIBs due to critical drawbacks. Firstly, its electronic conductivity (10^{-9} S cm^{-1}) is poorer than that for the conventional positive electrode materials (for instance, $>10^{-5}$ S cm^{-1} for $LiCoO_2$), which is due to the presence of an insulating Li_2MnO_3 phase.[8,9] For the practical use of this multi-component oxide material in LIBs, a large amount of conductive carbon over 10%, sometime over 20% in weight, is needed to keep proper electronic conductivity in the electrode.[21-23] But such a large amount of conducting agent could not be applicable for practical LIBs because it causes the falling off of energy density in the electrode. Secondly, electrolyte decomposition and film deposition are problematic since the commonly used electrolytes are not electrochemically stable under the working voltage of OLO (>4.4 V vs. Li/Li^+).[24-27] Hence, OLO surface should be passivated to avoid those parasitic reactions. Otherwise, resistive surface films continue to grow and enlarge electrode polarization that eventually leads to capacity fading.[28-35]

This work was motivated by the premises that carbon coating on OLO surface can solve the above-mentioned two problems; poor electronic conductivity and parasitic reactions. Normally, a conductive carbon powder is added as a physical mixture with electrode materials to compensate the poor bulk electronic conductivity of electrode materials. The role of conductive carbon is not to enhance the bulk electronic conductivity of electrode materials but to minimize the contact resistance by providing the electron transfer channel from current collector to the particles of a given electrode material. Unfortunately, this approach seems not viable for OLO electrode since a large amount of conductive carbon powder is needed for OLO electrodes. Namely, a larger number of contact points between OLO/OLO particles and OLO/current collector are needed to compensate the poor bulk electronic conductivity of OLO, which causes a decrease in volumetric energy density of LIBs due to the larger volume occupied by the passive component (carbon powder). In contrast, if carbon is added as a coating, the electron transfer channel can be provided with a minimal amount of carbon. Note that the contact area between OLO and coated carbon is greatly enlarged due to an intimate contact made between two components. As a result, the contact resistance at OLO/OLO particles and OLO/current collector can be effectively reduced. The second problem, which is the growth of film resistance as a result of persistent electrolyte decomposition, can also be mitigated by the carbon coating since the coated carbon can block the surface sites that are responsible for oxidative electrolyte decomposition.[36,37]

In this work, a novel highly conducting carbon coating procedure is developed for oxide positive electrode material, OLO, which is carried out at ambient temperature. The operational principle is simple; a controlled shear stress is continuously applied to the mixture of OLO powder and multi-walled carbon nanotubes (MWCNTs) in a specially designed mill. This work demonstrates, for the first time to our knowledge, that the carbon nanotubes can be uniformly coated on OLO surface by this method, and the performances of OLO positive electrode can be greatly improved by solving or at least mitigating the above-mentioned two problems.

2. Experimental

Material preparation

$Li_{1.17}Ni_{0.17}Co_{0.1}Mn_{0.56}O_2$ was prepared by oxalate co-precipitation and heat treatment at 900 °C for 12 h in air.[28] The obtained OLO powder was mixed with MWCNTs (E-nanotec, L-purified MWNT, length: 5–15 μm) by using a pestle and mortar. The controlled amount of MWCNT which were weight percent (wt.%) of 0.5, 1, 2, 3.5 and 5 against the OLO powder was used for sample preparation. The coating was performed at ambient temperature in a Nobilta mini bowl (Hosokawa, Japan), in which a rotating four-way blade is placed with 5 mm gap to the wall. A controlled shear stress was continuously applied to the mixture of MWCNTs and OLO powder within the gap by rotating the blade at 3000 rpm. The bowl was placed for the rotating axis to be parallel to the ground, with which the two components can be homogeneously mixed by using the effect of gravity.

Material Characterization: XRD analysis was carried out using an X'pert pro (PANalytical) diffractometer with Cu Kα radiation (1.54056). Raman spectra were obtained in backscattering mode using a Renishaw inVia system with an argon laser (514.5 nm). The XPS data were obtained using a Physical Electronics (PHI) (quantum 2000 scanning ESCA microprobe) spectrometer. The photoelectrons were excited with an Al Kα (1486.6 eV) anode operating at a constant power of 100 W (15 kV and 10 mA) with an X-ray spot size of 400 μm. The electronic conductivity of the electrode was measured using a 4-probe DC method under 20 kN and 90 kV (MCP-PD511, Mitsubishi).

Electrochemical analyses

For the preparation of the composite electrode, a slurry of the prepared sample, Denka black, and poly(vinylidene fluoride) (weight ratio of 94:3:3) was coated on an aluminum current collector. Total amount of carbon including MWCNT coated on OLO and Denka black was controlled to 3 wt.%. The electrode was then pressed to enhance the interparticle contact. Coin-type cells for both lithium half cells and full cells (2032 size,

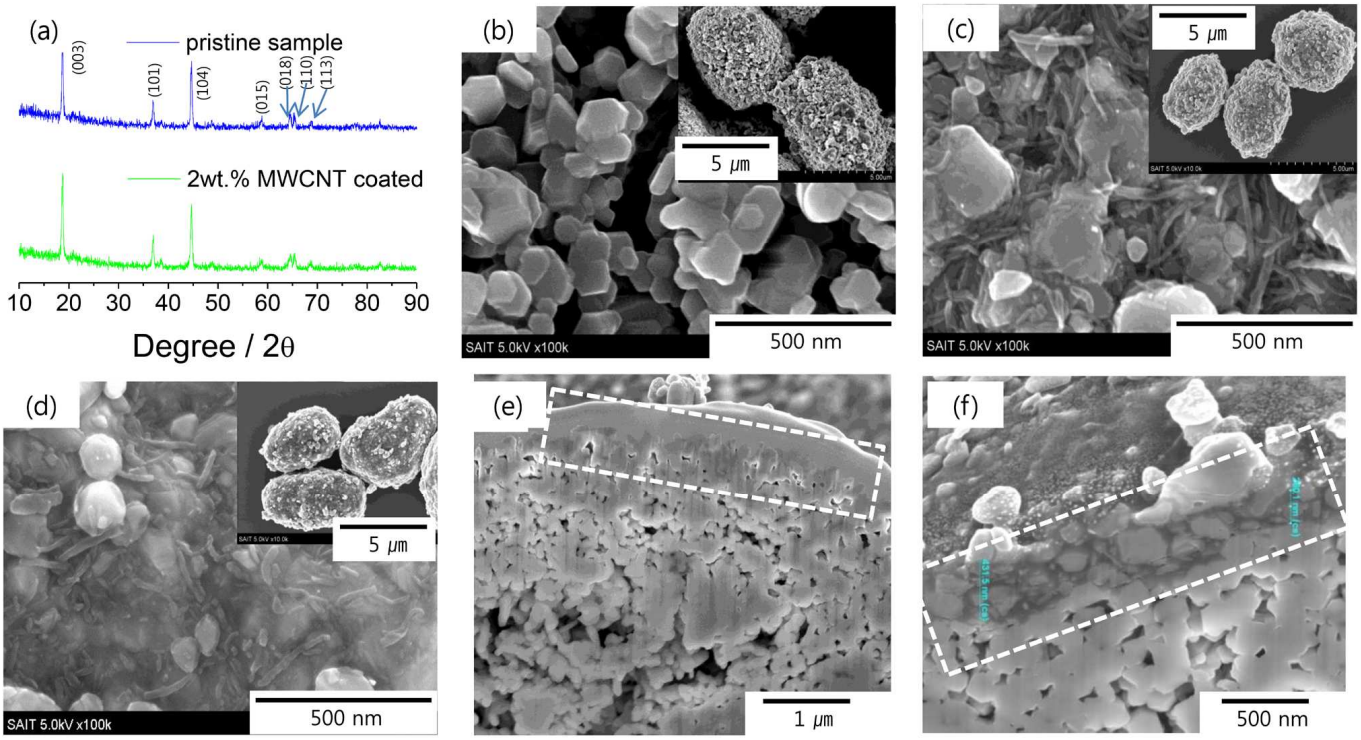

Fig. 1. (a) XRD patterns of the pristine and 2 wt. % MWCNT-coated (coating time = 20 min) OLO powders. FE-SEM top views of (b) pristine, (c) MWCNT-coated (coating time = 3 min) and (d) MWCNT-coated (coating time = 20 min). Cross-sectional FE-SEM images of (e) pristine and (f) MWCNT-coated (coating time = 20 min) OLO (Surface region is highlighted by rectangles with white dotted line.

Hohsen) were assembled with the composite electrode, a separator (Celgard), and a counter electrode. A lithium metal disk was used as the counter electrode for the lithium half cell and a composite electrode of graphite was used for the full cell. Galvanostatic cycling was carried out at 12.25 mA g^{-1} (0.1 C, 1 C = 245 mA g^{-1}) for cycle one, with subsequent cycling at 245 mA g^{-1} over the potential range 2.5–4.6 V (vs. Li/Li^{+}) for lithium half cells and 2.0–4.55 V for full cells (model TOSCAT 3500U) at 25 °C.

3. Results and discussion

As shown in Fig S1, a controlled shear stress was applied between mixture of MWCNTs and the OLO powder (average secondary particle size = 5 μm) by using a rotating blade, resulting in coating of the cathode material with the MWCNTs. . With a top view, in the bowl of Nobilta mini instrument, a rotating four-way blade was designed with almost touching the wall of bowl with 5mm-gap (Figure S2a). During the blade-rotating with an aimed speed (3000 rpm), the controlled shear stress was continuously given to the surface of the mixture of OLO powder and the MWCNTs in the prepared 5mm-gap. After applying the shear stress, the MWCNT coated OLO was obtained because the smaller powder (the MWCNTs) began aggregating the surface of the larger powder (the OLO). And furthermore, those powders were coated homogeneously by leaning the bowl perpendicularly for that the rotating axis was parallel to the ground, with enabling to mix the powder each other by gravity (Figure S2b).

Figure 1a shows the X-ray diffraction (XRD) pattern of the prepared samples. The MWCNT-coated OLO powder sample gives the diffraction peaks belonging to the pristine OLO without additional peaks, indicative of no change in the OLO crystal structure during the coating process. This must be due to the low-temperature coating process without carbothermal reduction. Also, the scanning electron microscopy (SEM) images illustrate that the apparent particle morphology does not change. The secondary OLO particles, which are formed by aggregation of nanometer-sized primary particles, are not broken, reflecting that the applied shear stress is not strong enough to damage the secondary particles as well as the primary particles (insets of Figures 1b and 1c). Carbon coating can, however, be confirmed by inspecting the high-resolution field-emission scanning electron microscopy (FE-SEM) images. As seen in Figure 1c and 1d, the coated OLO particles carry the MWCNTs on their surface. Between those samples, the coating of MWCNTs improves as coating time increases from 3 to 20 minutes. Carbon coating is further confirmed by inspecting the cross sectional images. The surface region of pristine OLO appears clean without any foreign materials (Figure 1e). However, the coated sample carries a homogeneous ca.100-nm-thick MWCNT layer on its surface (Figure 1f).

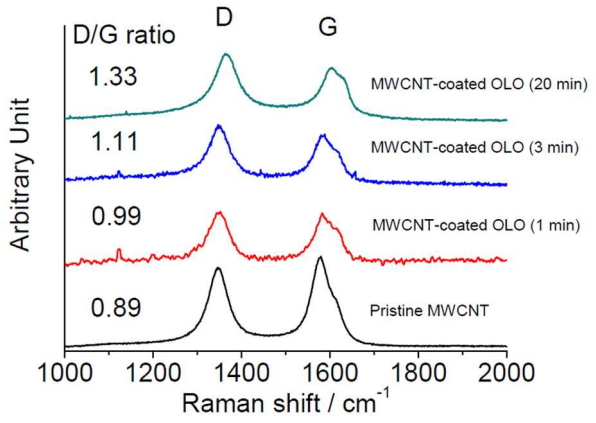

Fig 2. Raman spectra obtained from the pristine MWCNT and MWCNT-coated OLO samples. The coating time and calculated D/G ratio are indicated in the inset.

Even if the OLO particles are robust enough against the applied shear stress in this work, it is likely that the MWCNTs are prone to damage because they have a tube-type morphology and high aspect ratio to be broken more easily than the round-shaped OLO particles. This feature is ascertained by Raman analysis that was performed as a function of coating time (Figure 2). The pristine MWCNTs give two characteristic Raman peaks that come from the disordered carbon structure (D peak, 1350 cm^{-1}) and the ordered graphitic structure (G peak, 1590 cm^{-1}).[38] Although it is hard to observe D peak (A_1' symmetry vibration of carbons) in the crystal of graphite owing to its perfect symmetry, the number of defects on MWCNT increases the intensity of D peak. Oppositely, G peak (E_{2g} symmetry vibration of carbons) is generated from the in-plane vibration of the graphene layers and decreases as the site of defect interferes the vibration. The MWCNTs that were suffered from the applied shear stress for a longer period of time show an increase in the D peak at the expense of the G peak (from 0.89 to 1.33 in the D/G ratio), which must be due to cleavage of MWCNTs and conversion of the ordered graphene structure into the disordered amorphous state.

The coverage of MWCNTs on OLO surface is assessed by using X-ray photoelectron spectroscopy (XPS) as a function of coating time. The C 1s, O 1s, and Mn 2p XPS spectra are presented in Figures 3. As seen in the C 1s spectra, the

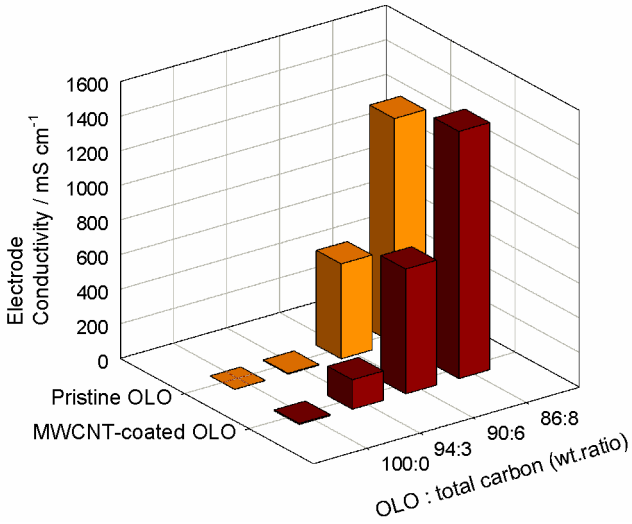

Fig 4. Electronic conductivity of the composite electrodes prepared from the pristine and MWCNT-coated OLO (coating time = 20 min) powders. Total carbon amount including MWCNT and Denka black was controlled to each wt. ratio by adding Denka black.

MWCNT-coated OLO sample shows a peak at 285 eV, which is assigned to the C 1s photoelectrons emitted from C–C moiety.[17,27,35] This peak becomes stronger, indicative of thicker or more uniform coverage of MWCNTs with an increase in coating time. The MWCNT-coated OLO samples also give the weak peaks at 286 eV (C–O or defects on carbon) and 289 eV (CO_3^{2-}).[17,27,35] This feature explains that the surface of MWCNTs is partially oxidized or defects form during the coating process. Thicker or more uniform carbon coverage with an increase in coating time is also confirmed from the O 1s and Mn 2p spectra. The O 1s photoelectrons at 529.5 eV and 531.5 eV, which are emitted from the oxide lattice in OLO, become less intense with an increase in coating time.[17,27,35] Similarly, the intensity of Mn $2p_{3/2}$ (642 eV) and Mn $2p_{1/2}$ (654 eV) photoelectrons that are emitted from Mn^{4+} ions in OLO becomes weaker with an increase in coating time since a thicker or more uniform carbon layer is coated on the OLO surface. In short, a high coverage of MWCNT is achieved by using the simple physical coating method. The relative atomic

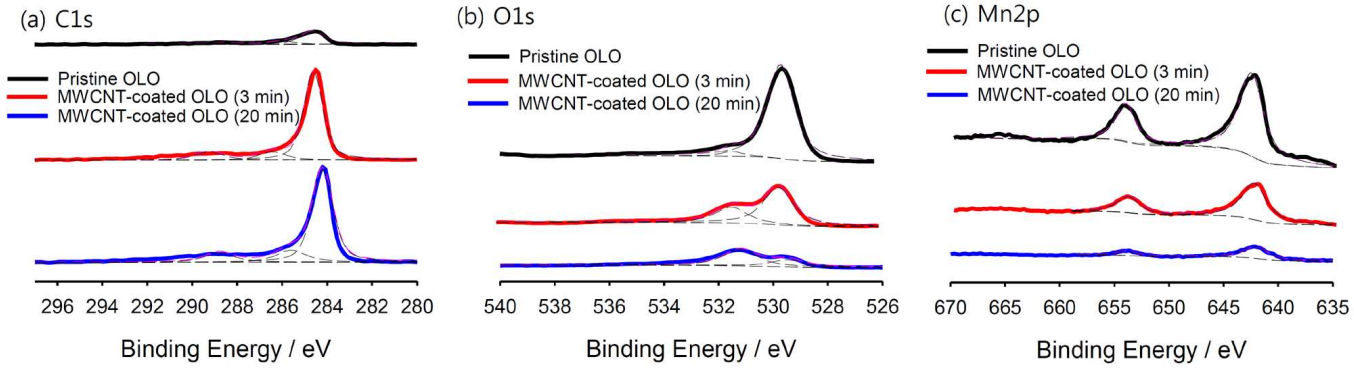

Fig. 3. XPS spectra of (a) C 1s, (b) O 1s, and (c) Mn 2p obtained from the pristine and MWCNT-coated samples. The fitted curves are indicated by the dotted lines.

concentration for each element is summarized in Table S1, in which it is seen that the atomic concentration of carbon amounts to 75.2 % after 20-min coating. In short, a high level of MWCNT coverage is achieved by using the simple physical coating method.

In order to confirm the role of coated MWCNT on OLO, which is expectedly the mitigation of contact resistance by providing the electron transfer channel, electronic conductivity was measured for the composite electrodes prepared from the pristine and MWCNT-coated OLO. To simulate the real electrode preparation, a conductive carbon powder (Denka black) was added, but the total amount of carbon (sum of Denka black and MWCNTs) was fixed at the predetermined values for a fair comparison. As shown in Figure 4, the electrodes prepared from the MWCNT-coated OLO show higher electronic conductivity in every composition. When the carbon loading is high (86:8), the conductivity difference is only marginal (1300 mS cm^{-1} for the pristine OLO and 1429 mS cm-1 for the MWCNT-coated OLO), probably due to the fact that the Denka black particles fill almost all the void spaces between the OLO particles. However, the conductivity difference becomes substantial with a decrease in the loading of total carbon. For instance, when the OLO: total carbon ratio is 94:3, the electronic conductivity is 170 mS cm^{-1} for the MWCNT-coated OLO and 4 mS cm^{-1} for the pristine OLO. In this carbon-depleted composition, the contact resistance should be high for the pristine OLO because the contact area between OLO and carbon particles is small. In the case of MWCNT-coated OLO, the contact area is already large enough, such that high electrode conductivity can be achieved even if the loading of Denka black is low.

Figure S3 exhibits the initial coulombic efficiencies and rate capabilities with varying amounts of MWCNT coating. Below 2 wt% MWCNT, the initial coulombic efficiency and rate capability of 2 C/0.2 C continuously increased with increasing amount of carbon. In a previous report, the discharge polarization was found to be high compared to charge sequence, and furthermore, the 1st coulombic efficiency can be improved

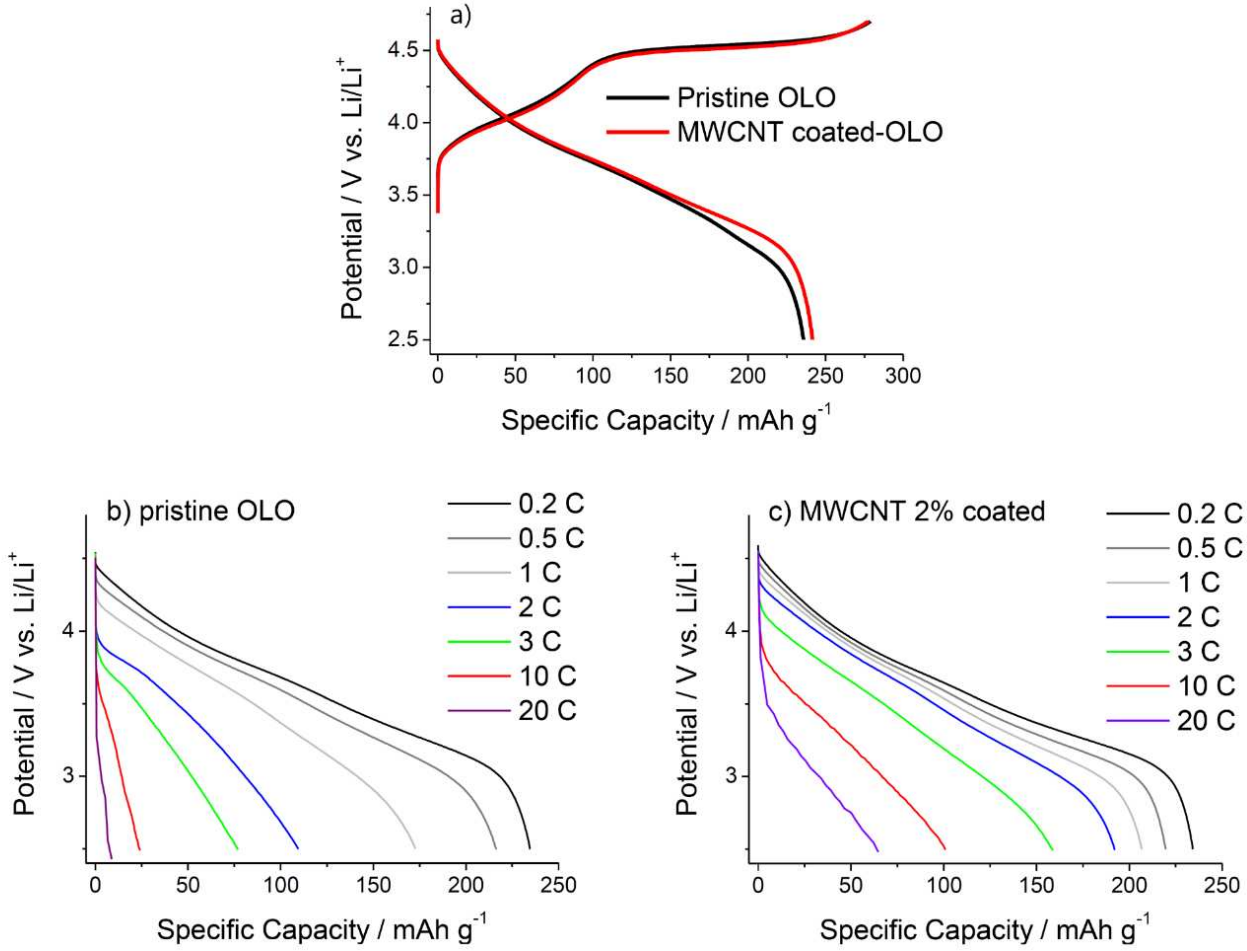

Fig. 5 (a) First voltage profiles obtained from lithium half cells with pristine and 2 wt% MWCNT-coated OLO. Current density: 2.45 mA g^{-1} (0.1 C); voltage cut-off: 2.5-4.7 V (vs. Li/Li^+); Discharge voltage profiles from the same cell with (b) pristine and (c) 2 wt% MWCNT-coated OLO with various discharge current densities after the controlled charge sequence (current density: 0.5 C; constant voltage mode was added to the end of charge until 0.05 C).

over 90% by controlling testing temperatures via room temperature-charge and high temperature discharge to lower kinetic parameter during discharging.[6,39] It was believed that the enhanced conductivity lowered the polarization during discharge and increased the discharge capacity, obtaining an improved initial coulombic efficiency. More badly, OLO needs to be charged over 4.4 V vs. Li/Li+ to enhance the obtained specific capacity with using the lithium ions in Li2MnO3. Under those highly oxidative conditions, the unfavorable electrolyte side reaction is accelerated on the surface of OLO. From these, it is also guessed that high coulombic efficiency is originated from that electrochemically stable carbon coating blocks the unfavorable side reaction of the electrolyte on the surface of OLO. Here, above 2 wt% MWCNT, there was no further improvement and so the amount of carbon was set to this concentration.

Figure 5a compares the charge/discharge voltage profiles obtained from the Li/pristine OLO and Li/ MWCNT-coated OLO cell in the first cycle. The specific capacity for both charging and discharging is comparable for two electrodes. The similarity in the latent capacity in turn illustrates that the OLO crystal structure is not changed during the coating due to the low-temperature process without carbothermal reduction, in agreement with the XRD results (Fig. 1a). In contrast, the specific discharge capacity for using the lithium ion batteries was higher in the case of the MWCNT-coated sample (bare: 234.8 and MWCNT-coated sample: 241.5 mAh g^{-1}). With considering that the higher discharge capacity of the MWCNT-coated sample, the improved conductivity relieved kinetic hindrances that restrict the discharge capacity especially at the end of discharge under 3.6 V, relating with the lithiation process into the activated MnO_2 from the Li_2MnO_3 during the 1st charge sequence over 4.4 V.

The rate capability is compared for two electrodes in the discharging sequence in Figures 5b and c. Clearly, the MWCNT-coated OLO outperforms the pristine one. For instance, the discharge capacity obtained at 10 C (2450 mA g^{-1}) amounts to 103 mAh g^{-1} for the coated electrode, but it is only 24 mAh g^{-1} for the pristine one. The discharge voltage profiles shown in Fig. 5b and 5c reveal that the contact resistance at the OLO/OLO particles has a strong effect on the rate property. Namely, two electrodes show a big difference in the Ohmic resistance that appears as a vertical potential drop at the very early period of discharge. When the OLO electrodes are discharged at the slower rates (0.2~0.5C), the electrode potential drop is marginal and comparable for two electrodes. When the rate is increased, however, the potential drop itself becomes larger and the difference of potential drop becomes larger for two electrodes. At 10 C, for instance, the potential of pristine OLO electrode drops down to 3.5 V right after the cell being discharged, whereas the potential of coated OLO electrode remains at 3.9 V at the same discharge rate. The shape of voltage profile as well as the Ohmic resistance also altered by MWCNT-coating. Especially, the plateaus between 3.5 and 3.0 V highly improved by MWCNT-coating. With the pristine sample, it means that the effect of these resistive behaviours becomes more serious under high current condition than that under the moderate current condition. These severe obstacles were higly relived by MWCNT-coating on OLO.

To investigate the resistance behaviour in more detail, AC impedance analysis at various stages of lithiation and delithiation was carried out. The AC impedance results obtained from 3-electrode cells; comprising the prepared electrode as the working electrode and two lithium electrodes as the counter and reference electrodes, exhibit some differences. Two semicircles can be clearly observed in Figures 6; diameter of the semicircle at high frequency correspond to the resistance of the surface film resistance and that at low frequency correspond to the charge-transfer resistance of lithium reactions occurring on the electrode surface.[38] The impedance results were fitted with the equivalent circuit shown in Figure 6a. The most revealing feature in Figures 6a-c is that both the semicircles of the MWCNT-coated OLO are always

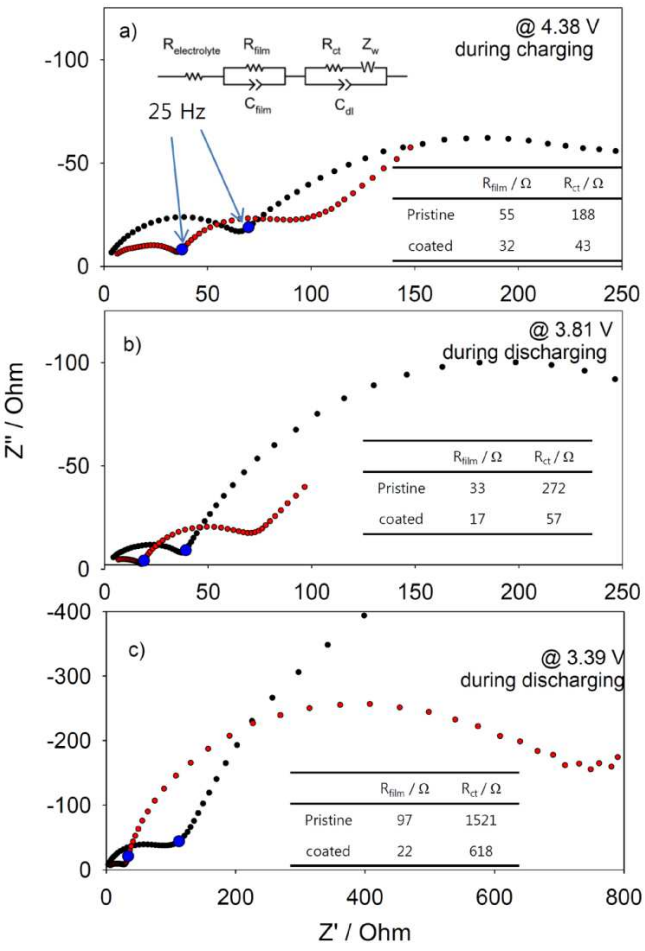

Fig. 6 AC impedance spectra (as a Nyquist) obtained with the 3-electrode cell with pristine (black square) and 2 wt% MWCNT-coated OLO (red square) (a) at the 4.38 V during the 1st charging, (b) at the 3.81 V and (c) at the 3.39 V during the 1st discharge at 25 °C. The proposed equivalent circuit for fitting is depicted on the left upper. Each fitted values of Rfilm and Rct are shown.

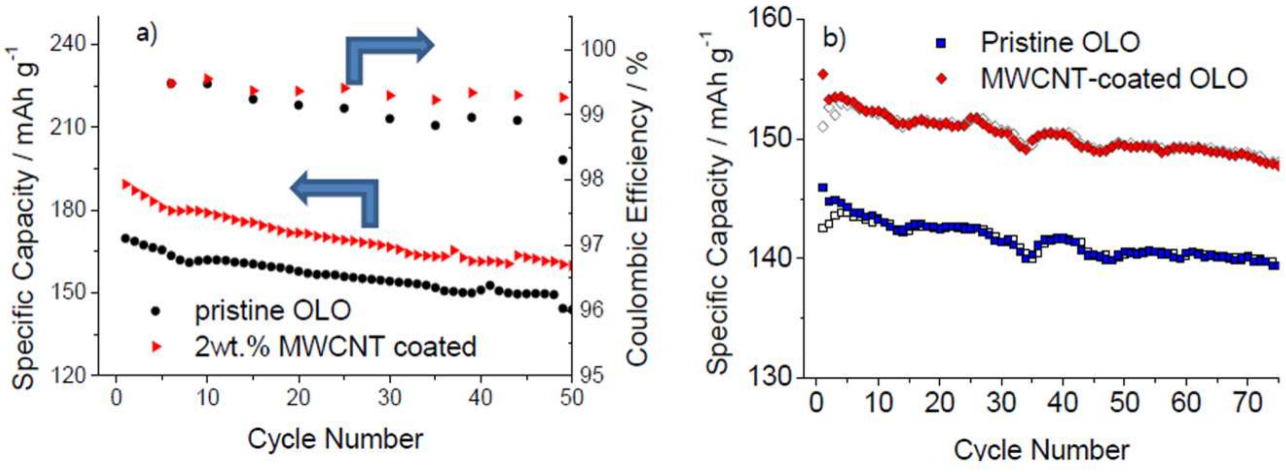

Fig. 7 (a) The obtained cyclability and Coulombic efficiency (average of 5 cycles) from the half cell with pristine and 2 wt% MWCNT-coated samples; (b) cyclability of the full cell with pristine and 2 wt% MWCNT-coated sample with constant charge and discharge current (1 C) at ambient temperature.

smaller than those of the pristine OLO, demonstrating that the kinetic hindrances were alleviated. It is speculated this was due to the enhanced surface stability and electronic conductivity of the electrode owing to the MWCNT-coating. It also improved the kinetic characteristics of charge-transfer resistance by increasing the active sites for electrochemical reaction without isolating the active material. In more detail on the pristine OLO, as lithiation proceeded after the 1st charging, the high frequency-circle in the Nyquist plot obtained during discharging decreased at 3.81 V but increased again at 3.39 V on further discharging owing to insulation caused by surface-film deposition of materials such as Li_2CO_3 and Li_2O from electrolyte decomposition or oxidation by oxygen from OLO.[37,40] The behaviour of the low frequency-circle is also similar with that of the high frequency circle. The charge-transfer resistances increased greatly at the end of discharge sequences, corresponding to sluggish delithiation and lithiation reactions owing to surface film.[17,26] The resistance during the discharge is much larger than those during the charge. Unlike the pristine OLO, the film resistance of the MWCNT-coated OLO during discharge, however, decreased from 32 to 22 Ω. The high resistive behaviour of the OLO on the discharging was also greatly relieved by MWCNT-coating. It agreed with that the polarization was highly reduced during the discharge sequence in the voltage profiles (Figure 5a) and rate capability test (Figure 5b and c).

The cyclability was found to be reasonable after coating with MWCNT, with the obtained capacity being >180 mAh g^{-1} even for the 94:3 electrode composition. The specific capacity achieved for the MWCNT-coated electrode was higher than that of the pristine sample; the average coulombic efficiency during 50 cycles (2wt% MWCNT-coated OLO: 99.5%) was also higher than that for the pristine samples (99.1%) (Figure 7a). It is speculated that the surface carbon coating additionally blocked the continuous electrolyte decomposition on the cathode under oxidative conditions at high potential.

Finally, we fabricated full cells using the prepared cathode samples and a graphite anode. A full cell with the 2 wt% MWCNT-coated OLO exhibited a higher discharge capacity, exceeding 150 mAh g^{-1} (divided by the mass of OLO), than that containing the pristine sample at a constant current/constant voltage rate of 245 mAh g^{-1} between 2.5 and 4.6 V at 25 °C. Importantly, the obtained cyclability was highly stable even after 70 cycles (Figure 7b).

4. Conclusions

MWCNT coating on the OLO cathode material introduced here is the first system that has been reported to overcome the kinetic hindrances of poor initial coulombic efficiency and rate capability. We confirmed that MWCNT coating could be successfully achieved by a simple physical coating method without any breakdown in cathode structure. These improvements have great potential for producing improved lithium ion batteries, because the methodology could be used for various different cathode materials, without damaging their original crystal structure. These results pave the way for highly conductive MWCNT coatings on oxide cathode materials..

Acknowledgements

The acknowledgements come at the end of an article after the conclusions and before the notes and references.

Notes and references

[a] Energy Laboratory, Samsung Advanced Institute of Technology, Samsung Electronics Co Ltd., 130 Samsung-ro, Suwon, Gyeonggi-do 443-803 (Republic of Korea).

[b] Department of Energy and Chemical Engineering, Incheon National University, 119 Academy-ro, Songdo-dong, Yeonsu-gu, Incheon 406-772 (Republic of Korea)
[c] Center for Energy Convergence, KIST, Hwarangno 14gil 5Seongbuk-gu 136-791 (Republic of Korea)

† Footnotes should appear here. These might include comments relevant to but not central to the matter under discussion, limited experimental and spectral data, and crystallographic data.

Electronic Supplementary Information (ESI) available: [details of any supplementary information available should be included here]. See DOI: 10.1039/b000000x/

1 M. Gu, I. Belharouak, J. Zheng, H. Wu, J. Xiao, A. Genc, K. Amine, S. Thevuthasan, D. R. Baer, J. G. Zhang, N. D. Browning, J. Liu and C. Wang, ACS Nano, 2013, **7**, 760.
2 Jeong, Y.-U. Kim, H. Kim, Y.-J. Kim and H.-J. Sohn, *Energ. Environ. Sci.*, 2011, **4**, 1986.
3 Y. K. Sun, S. T. Myung, B. C. Park, J. Prakash, I. Belharouak and K. Amine, *Nat. Mater.*, 2009, **8**, 320.
4 Y.-S. Kang, T. Yoon, J. Mun, M. S. Park, I.-Y. Song, A. Benayad and S. M. Oh, *J. Mater. Chem. A*, 2014, **2**, 14628.
5 Y.-K. Sun, M.-J. Lee, C. S. Yoon, J. Hassoun, K. Amine and B. Scrosati, *Adv. Mater.*, 2012, **24**, 1192.
6 K. J. Rosina, M. Jiang, D. Zeng, E. Salager, A. S. Best and C. P., *J. Mater. Chem.*, 2012, **22**, 20605.
7 W. Choi, A. Benayard, J.-H. Park, J. Park, S.-G. Doo and J. Mun, *Electrochim. Acta*, 2014, **117**, 492.
8 A. Ponrouch, A. R. Goñi, M. T. Sougrati, M. Ati, J. M. Tarascon, J. Nava-Avendaño and M. R. Palacín, *Energ. Environ. Sci.*, 2013, **6**, 3363.
9 H. Li and H. Zhou, *Chem. Commun.*, 2012, **48**, 1201.
10 J. Liu, Q. Y. Wang, B. Reeja-Jayan and A. Manthiram, *Electrochem. Commun.*, 2010, **12**, 750-753.
11 Q. Cao, H. P. Zhang, G. J. Wang, Q. Xia, Y. P. Wu and H. Q. Wu, *Electrochem. Commun.*, 2007, **9**, 1228.
12 S. Luo, K. Wang, J. Wang, K. Jiang, Q. Li and S. Fan, *Adv. Mater.*, 2012, **24**, 2294-2298.
13 A. Varzi, D. Bresser, J. von Zamory, F. Müller and S. Passerini, *Adv. Energy Mater.*, DOI 10.1002/aenm.201400054
14 P. Manikandan, P. Periasamy and R. Jagannathan, *J. Mater. Chem. A*, 2013, **1**, 15397.
15 Y. Zhou, J. Wang, Y. Hu, R. O'Hayre and Z. Shao, *Chem. Commun.*, 2010, **46**, 7151.
16 B. Li, H. Yan, J. Ma, P. Yu, D. Xia, W. Huang, W. Chu, Z. Wu, Adv. Funct. Mater. DOI 10.1002/adfm.201400436.
17 N. Yabuuchi, K. Yoshii, S. T. Myung, I. Nakai, S. Komaba, *J. Am. Chem. Soc.*, 2011, **133**, 4404.
18 K.-S. Park, D. Im, A. Benayad, A. Dylla, K. J. Stevenson, J. B. Goodenough, *Chem. Mater.*, 2012, **24**, 2673.
19 J. Bareno, C. Lei, J. Wen, S. H. Kang, I. Petrov, D. Abraham, *Adv. Mater.* 2010, **22**, 1122.
20 M. G. Kim, J. Cho, *Adv. Funct. Mater.,* 2009, **19**, 1497.
21 D. Wang, I. Belharouak, G. Zhou and K. Amine, *Adv. Funct. Mater.*, 2013, **23**, 1070.
22 Y. K. Sun, Z. Chen, H. J. Noh, D. J. Lee, H. G. Jung, Y. Ren, S. Wang, C. S. Yoon, S. T. Myung and K. Amine, Nat. Mater., 2012, **11**, 942.
23 D. Mohanty, S. Kalnaus, R. A. Meisner, K. J. Rhodes, J. Li, E. A. Payzant, D. L. Wood Iii and C. Daniel, *J. Power Sources*, 2013, **229**, 239.
24 A. Van Bommel, J. R. Dahn, *Electrochem. Solid-State Lett.*, 2010, **13**, A62.
25 Z. Li, F. Du, X. Bie, D. Zhang, Y. Cai, X. Cui, C. Wang, G. Chen, Y. Wei, *J. Phys. Chem. C*, 2010, **114**, 22751.
26 M. Jiang, B. Key, Y. S. Meng, C. P. Grey, *Chem. Mater.*, 2009, **21**, 2733.
27 S. K. Martha, J. Nanda, G. M. Veith, N. J. Dudney, *J. Power Sources,* 2012, **216**, 179.
28 K.-S. Park, A. Benayad, M.-S. Park, W. Choi, D. Im, *Chem. Commun.*, 2010, **46**, 4190.
29 H. K. Song, K. T. Lee, M. G. Kim, L. F. Nazar, J. Cho, *Adv. Funct. Mater.*, 2010, **20**, 3818.
30 E. S. Lee, A. Manthiram, *J. Electrochem. Soc.*, 2011, **158**, A47.
31 S. H. Kang, M. M. Thackeray, *Electrochem. Commun.*, 2009, **11**, 748.
32 B. Liu, Q. Zhang, S. He, Y. Sato, J. Zheng, D. Li, *Electrochim. Acta*, 2011, **56**, 6748.
33 Y. S. Park, K. H. Choi, H. K. Park, S. M. Lee, *J. Electrochem. Soc.*, 2010, **157**, A850.
34 Y. S. Jung, P. Lu, A. S. Cavanagh, C. Ban, G.-H. Kim, S.-H. Lee, S. M. George, S. J. Harris, A. C. Dillon, *Adv. Energy Mater.*, 2012, **3**, 213.
35 J. Mun, S. Kim, T. Yim, J. H. Ryu, Y. G. Kim, S. M. Oh, *J. Electrochem. Soc.*, 2010, **157**, A136.
36 M. Noh, Y. Kwon, H. Lee, J. Cho, Y. Kim, M. G. Kim, *Chem. Mater.* 2005, **17**, 1926.
37 J. Wolfenstine, J. Read, J. Allen, *J. Power Sources,* 2007, **163**, 1070.
38 J. Mun, T. Yim, S. Jurng, J. H. Park, S. Y. Lee, J. H. Ryu, Y. G. Kim, S. M. Oh, *Electrochem. Commun.*, 2011, **13**, 1256.
39 B. Qiu, J. Wang, Y. Xia, Z. Wei, S. Han and Z. Liu, *J. Power Sources*, 2014, **268**, 517.
40 H. Yu, Y. Wang, D. Asakura, E. Hosono, T. Zhang, H. Zhou, *RSC Adv.* 2012, **2**, 8797.

For high rate capability and energy density of lithium ion batteries, over-lithiated layered cathodes coated by multiwall carbon nanotube were prepared by novel dry method without structure decaying.